RESEARCH ARTICLE

Protein microarray analysis of cytokine expression changes in distal stumps after sciatic nerve transection

Xiao-Qing Cheng[1, #], Xue-Zhen Liang[1, 2, #], Shuai Wei[1, #], Xiao Ding[1], Gong-Hai Han[1], Ping Liu[1], Xun Sun[1], Qi Quan[1], He Tang[1], Qing Zhao[1], Ai-Jia Shang[3, 4, *], Jiang Peng[1, 3, *]

1 Beijing Key Laboratory of Regenerative Medicine in Orthopedics, Institute of Orthopedics, Chinese PLA General Hospital, Beijing, China
2 The First Clinical Medical College, Shandong University of Traditional Chinese Medicine, Jinan, Shandong Province, China
3 Co-innovation Center of Neuroregeneration, Nantong University, Nantong, Jiangsu Province, China
4 Department of Neurosurgery, Chinese PLA General Hospital, Beijing, China

Funding: *This study was supported by the National Key Research & Development Program of China, No. 2017YFA0104702 (to AJS), and the National Basic Research Program of China (973 Program), No. 2014CB542201 (to JP).*

Graphical Abstract

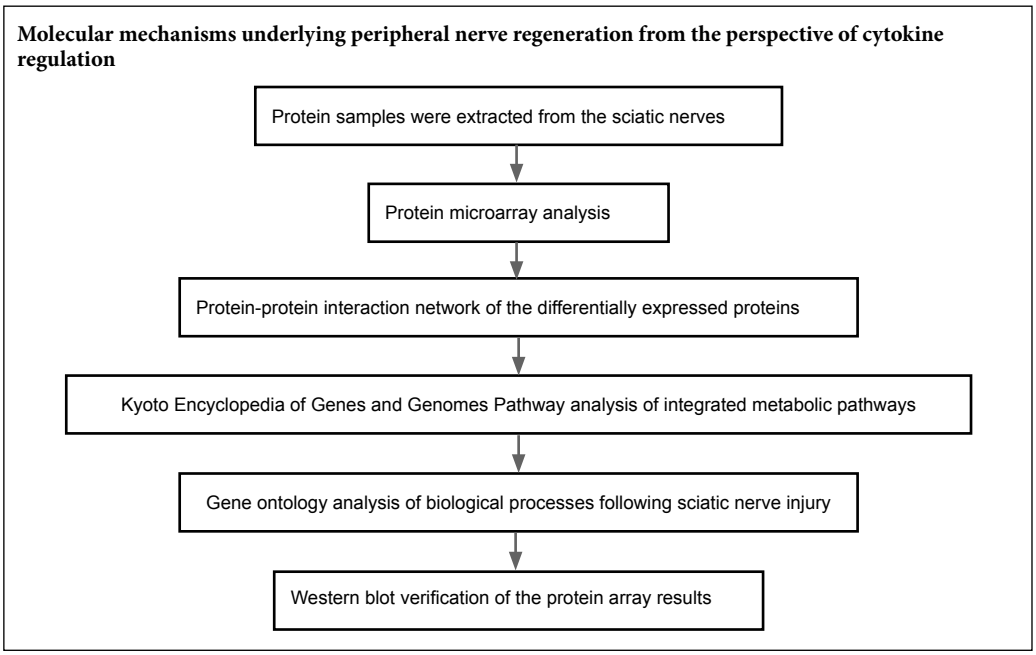

Correspondence to:
Ai-Jia Shang, shangaj@126.com;
Jiang Peng,
pengjiang301@126.com.

#These authors contributed equally to this work.

orcid:
0000-0003-4662-9288
(Jiang Peng)

doi: *10.4103/1673-5374.266062*

Received: *December 5, 2018*
Accepted: *March 8, 2019*

Abstract

A large number of chemokines, cytokines, other trophic factors and the extracellular matrix molecules form a favorable microenvironment for peripheral nerve regeneration. This microenvironment is one of the major factors for regenerative success. Therefore, it is important to investigate the key molecules and regulators affecting nerve regeneration after peripheral nerve injury. However, the identities of specific cytokines at various time points after sciatic nerve injury have not been determined. The study was performed by transecting the sciatic nerve to establish a model of peripheral nerve injury and to analyze, by protein microarray, the expression of different cytokines in the distal nerve after injury. Results showed a large number of cytokines were up-regulated at different time points post injury and several cytokines, e.g., ciliary neurotrophic factor, were downregulated. The construction of a protein-protein interaction network was used to screen how the proteins interacted with differentially expressed cytokines. Kyoto Encyclopedia of Genes and Genomes pathway and Gene ontology analyses indicated that the differentially expressed cytokines were significantly associated with chemokine signaling pathways, Janus kinase/signal transducers and activators of transcription, phosphoinositide 3-kinase/protein kinase B, and notch signaling pathway. The cytokines involved in inflammation, immune response and cell chemotaxis were up-regulated initially and the cytokines involved in neuronal apoptotic processes, cell-cell adhesion, and cell proliferation were up-regulated at 28 days after injury. Western blot analysis showed that the expression and changes of hepatocyte growth factor, glial cell line-derived neurotrophic factor and ciliary neurotrophic factor were consistent with the results of protein microarray analysis. The results provide a comprehensive understanding of changes in cytokine expression and changes in these cytokines and classical signaling pathways and biological functions during Wallerian degeneration, as well as a basis for potential treatments of peripheral nerve injury. The study was approved by the Institutional Animal Care and Use Committee of the Chinese PLA General Hospital, China (approval number: 2016-x9-07) in September 2016.

Key Words: *cytokines; distal stump; gene ontology; Kyoto Encyclopedia of Genes and Genomes pathway; peripheral nerve injury; protein microarray; protein-protein interaction network; Wallerian degeneration*

Chinese Library Classification No. *R447; R363; R741*

Introduction

Although the peripheral nerve has remarkable regenerative abilities after injury, it is difficult to recover completely from long-term nerve defects following peripheral nerve injury (PNI) (Raimondo et al., 2011). After PNI, Wallerian degeneration, a complicated process involving distal axonal degeneration and myelin breakdown, takes place immediately (Geuna et al., 2009). Subsequently, multiple macrophages and monocytes migrate to remove the axon and myelin debris. Schwann cells proliferate to form bands of Büngner as a bridge to the defective peripheral nerve system. They secrete a large number of chemokines, cytokines and other trophic factors and extracellular matrix molecules, which form a favorable microenvironment for peripheral nerve regeneration (Frostick et al., 1998; Chen et al., 2007). This microenvironment is one of the major factors of regenerative success (Webber and Zochodne, 2010). Therefore, it is important to investigate the key molecules and regulators affecting nerve regeneration after PNI.

In early studies, microarrays were widely used to characterize differentially expressed genes in the distal nerve stump following PNI (Pan et al., 2017). Temporal expression patterns of upregulated and downregulated genes during Wallerian degen-eration were validated (Yu et al., 2016; Yi et al., 2017). RNA-sequencing was also performed to evaluate comprehensive transcriptomic expression and identify numerous differentially expressed microRNAs at different time points during peripheral nerve regeneration (Yi et al., 2015). These studies have helped elucidate global gene expression changes involved in peripheral nerve repair. However, in many cases during peripheral nerve regeneration, multiple cellular events occur after a gene is translated into a protein. Several studies have suggested that some proteins have significant effects on many biological processes during peripheral nerve repair and Wallerian degeneration, including immune responses, macrophage recruitment and Schwann cell reprogramming (van der Laan et al., 1996; da Costa et al., 1997; Siebert et al., 2000; Takahashi et al., 2007; Clements et al., 2017). Nevertheless, the integrated relationships between proteins involved in PNI and recovery are not yet clear.

In this study, we aimed to investigate the dynamic differential expression of 67 cytokines using a protein micro-array to achieve greater insight into the relative pathways or networks during Wallerian degeneration of injured sciatic nerve. We used bioinformatic analyses (protein-protein interaction (PPI) network, Kyoto Encyclopedia of Genes and Genomes Pathway (KEGG) pathway and gene ontology (GO) analysis).

Materials and Methods

Animals

In this study, eighty male Sprague-Dawley rats (specific pathogen free level) weighing 200–250 g, aged 7–8 weeks, were obtained from the Experimental Animal Research Center at the Chinese PLA General Hospital, China. The rats were housed in a temperature-controlled environment and fed water and food *ad libitum*. The Institutional Animal Care and Use Committee of the Chinese PLA General Hospital, China approved the experimental procedures (approval No. 2016-x9-07) in September 2016.

Rats were randomly divided into five groups: control and 4 periods post injury. Briefly, rats were anesthetized by intraperitoneal injection of pentobarbital (30 mg/kg; Sigma-Aldrich, St. Louis, MO, USA). The sciatic nerve was exposed via incision on the lateral aspect of the right hind limb and was excised through the middle site of the exposed sciatic nerve (Yu et al., 2012). At 1, 7, 14, and 28 days after nerve transection, the rats were sacrificed by decapitation. The distal nerve stumps were removed and stored at −80°C until further use. As a control, rats in the 0 day group underwent sham surgery of the right sciatic nerves.

Protein microarray analysis

Protein samples were extracted from the distal nerve stumps of sciatic nerves of the rats and lysed in radioimmuno-precipitation assay buffer lysis buffer containing a protease inhibitor cocktail (Pulilai, Beijing, China). Subsequently, protein concentrations were determined using the Pierce Bicinchoninic acid assay Kit (Thermo Fisher, Waltham, MA, USA).

Microarray analysis was performed using the Rat Cytokine Array 67 (RayBiotech, Guangzhou, Guangdong Province, China), as described previously (Luck et al., 2017). Briefly, the microarray was incubated with 100 μL sample diluent at room temperature for 30 minutes to block the slides. After removing the diluent, the array was completely covered with 100 μL of the protein sample (2 mg/mL) and incubated at 4°C overnight. Biotinylated antibody cocktail (80 μL) was added to each well at room temperature for 2 hours. Cy3 equivalent dye-conjugated streptavidin (80 μL) was added to each well, and the wells were covered with aluminum foil and placed in a dark room to avoid light exposure at room temperature for 1 hour. The signals were visualized using the LuxScan 10K scanner (CapitaBio, Beijing, China) at 532 nm wavelength.

Bioinformatic analysis

The expression levels of proteins at 1, 7, 14, and 28 days after sciatic nerve transection were compared with those in the control group. Proteins with an expression fold change > 2 or < −2 and adjusted *P*-value < 0.05 were considered significantly differentially expressed. The differentially expressed proteins, Venn diagram and Principal Component analysis were performed by R packages (http://www.R-project.org) named gplots, VennDiagram and scatterplot3d, respectively. The GeneMANIA database (http://genemania.org) is a gene and protein analysis tool designed to predict PPIs. The various proteins were mapped using GeneMANIA to evaluate the interactive relationships among them. The PPI networks were then constructed using Cytoscape software (http://www.cytoscape.org).

Proteins selected from the PPI networks were systematically analyzed using the Database for Annotation, Visu-alization and Integrated Discovery (DAVID; http://www.da-

vid.niaid.nih.gov) program to identify significantly enriched KEGG pathways and GO categories (Dennis et al., 2003). The KEGG pathways and GO categories were performed by R packages named ggplot2.

Western blot analysis

Sciatic nerves were rinsed in cold PBS and lysed on ice in radioimmunoprecipitation assay buffer containing a protease inhibitor cocktail (Pulilai), and the resulting tissue lysates were mixed with sample buffer and boiled at 95°C for 5 minutes. Equal amounts of protein from each sample were subjected to 10–15% sodium dodecyl sulfate-polyacrylamide gel electrophoresis and transferred to polyvinylidene fluoride membranes (Pulilai). The membranes were blocked in 5% nonfat dry milk at 4°C for 1 hour and incubated with rabbit anti-hepatocyte growth factor (HGF) antibody (1:1000; ab83760, Abcam, Cambridge, UK), rabbit anti-glial cell line-derived neurotrophic factor (GDNF) antibody (1:1000; ab18956, Abcam), rabbit anti-ciliary neurotrophic factor (CNTF) antibody (1:1000; ab46172, Abcam) or rabbit anti-β-actin antibody (1:1000; Proteintech, Chicago, IL, USA) at 4°C overnight. These were followed by the appropriate secondary antibody, donkey-anti-rabbit-HRP (1:5000, Pulilai) at room temperature for 1 hour. The membranes were developed using an enhanced chemiluminescence substrate (Thermo Fisher). Measurement of the protein band intensities was conducted using ImageJ software (National Institutes of Health, Bethesda, MD, USA).

Statistical analysis

All data are expressed as the mean ± standard error of the mean (SEM). Significant differences among data were determined by one-way analysis of variance, followed by Tukey's *post hoc* test. All analyses were performed using GraphPad Prism 7.0 (GraphPad Software, Inc., San Diego, CA, USA) and a P-value < 0.05 was designated as indicating statistical significance.

Results

Differentially expressed proteins in the distal nerve stump following sciatic nerve transection

To gain a better understanding of the microenvironment of the distal nerve stump, we examined the expression patterns of 67 proteins in injured sciatic nerves at different time points using the Rat Cytokine Array 67 (**Table 1**). Proteins with a fold change in expression > 2 or < −2 and an adjusted $P < 0.05$ were defined as differentially expressed. A full list of the differentially expressed proteins at each time point evaluated is displayed in a heatmap (**Figure 1A–D**). Compared with the control group (0 day after PNI), the expression of nearly 20% of the total proteins increased at 1 day after PNI, including some chemokines and interleukins (ILs). The number of upregulated proteins increased to 33% of the total proteins at 7 days after PNI. In addition to chemokines and ILs, Notch 1/2 and Neuropilin 1/2, which are related to some classical pathways, increased in expression starting at 7 days after PNI. At 14 days after PNI, no ILs, except for IL-22, showed any remarkable expression changes. At 28 days after PNI, the number of upregulated proteins had decreased slightly. From day 1 to day 28 after PNI, only a few proteins, including CNTF, were downregulated. The numbers of overlapping differentially expressed proteins at 1, 7, 14, 28 days post injury are displayed in a Venn diagram (**Figure 1E**). Principal component analysis based on the expression values of the 67 proteins demonstrated five completely independent clusters: control and the other time points after injury (**Figure 1F**).

Table 1 The 67 cytokine proteins included on the RayBiotech Rat Cytokine Array 67

Proteins	Genes	Proteins	Genes	Proteins	Genes	Proteins	Genes
CD48	*Cd48*	IL-10	*Il10*	CNTF	*Cntf*	Adiponectin	*Adipoq*
B7-1	*Cd80*	IL-13	*Il13*	FGF-BP	*Fgfbp1*	RAGE	*Ager*
B7-2	*Cd86*	IL-17F	*Il17f*	GFR alpha-1	*Gfra1*	GM-CSF	*Csf2*
P-Cadherin	*Cdh3*	IL-1a	*Il1a*	HGF	*Hgf*	Decorin	*Dcn*
Eotaxin	*Ccl11*	IL-1b	*Il1b*	IFNg	*Ifng*	EphA5	*Epha5*
MCP-1	*Ccl2*	IL-1 R6	*Il1rl2*	b-NGF	*Ngf*	Erythropoietin	*Epo*
CTACK	*Ccl27*	IL-1 ra	*Il1rn*	PDGF-AA	*Pdgfa*	JAM-A	*F11r*
MIP-1a	*Ccl3*	IL-2	*Il2*	TNFa	*Tnf*	Gas 1	*Gas1*
RANTES	*Ccl5*	IL-22	*Il22*	VEGFA	*Vegfa*	TIM-1	*Havcr1*
Fractalkine	*Cx3cl1*	IL-2 Ra	*Il2ra*	4-1BB	*Tnfrsf9*	ICAM-1	*Icam1*
CINC-1	*Cxcl1*	IL-3	*Il3*	Flt-3L	*Flt3lg*	Nope	*Igdcc4*
CINC-3	*Cxcl2*	IL-4	*Il4*	Galectin-1	*Lgals1*	Activin A	*Inhba*
CINC-2	*Cxcl3*	IL-6	*Il6*	Galectin-3	*Lgals3*	SCF	*Kitlg*
LIX	*Cxcl5*	gp130	*Il6st*	Notch-1	*Notch1*	TCK-1	*Ppbp*
TIMP-1	*Timp1*	IL-7	*Il7*	Notch-2	*Notch2*	Prolactin	*Prl*
TIMP-2	*Timp2*	TWEAK R	*Tnfrsf12a*	Neuropilin-1	*Nrp1*	Prolactin R	*Prlr*
		TREM-1	*Trem1*	Neuropilin-2	*Nrp2*	L-Selectin	*Sell*

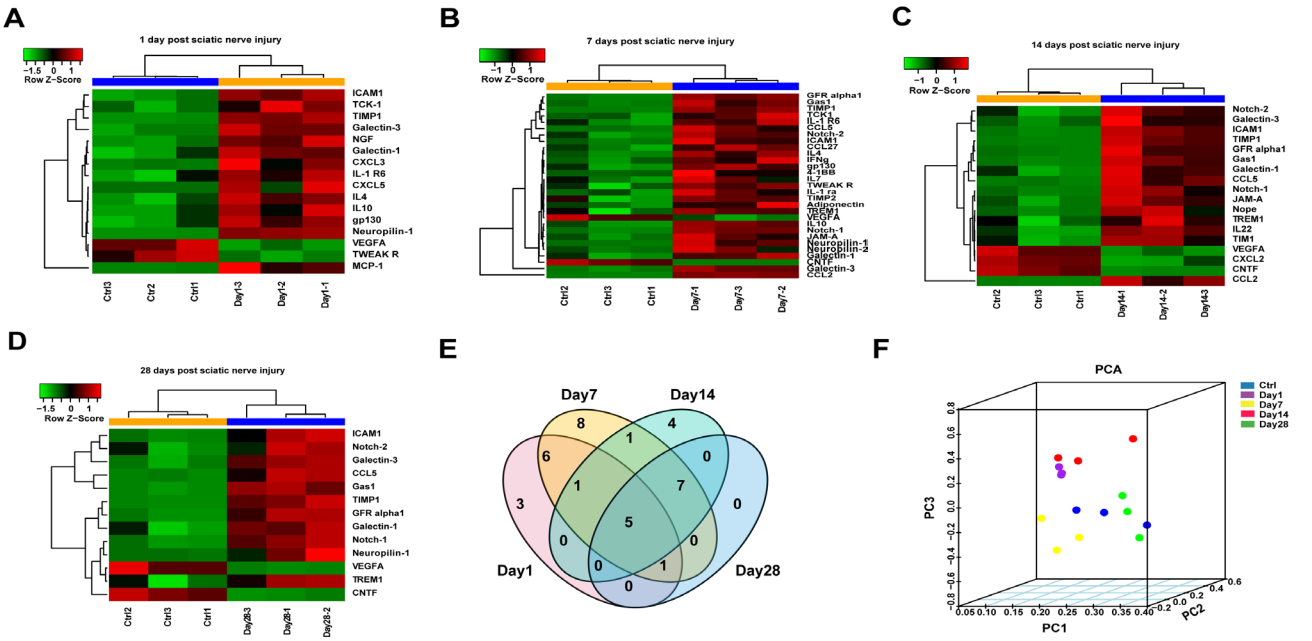

Figure 1 Overview of differentially expressed cytokines at the distal stump following sciatic nerve transection.
(A–D) Heatmap and hierarchical clustering at 1 (A), 7 (B), 14 (C), 28 (D) days. Protein expression was increased (red) and decreased (green) compared with the control (0 day after sciatic nerve transection). (E) Venn diagram displaying the number of different proteins among the four groups of sciatic nerves at each time point after sciatic nerve transection. (F) Principal component analysis of the differentially expressed cytokines at different time points following sciatic nerve transection. PC: Principal component; PCA: principal component analysis.

Protein-protein interaction network of the differentially expressed proteins

Many proteins were temporally differentially expressed in the injured sciatic nerve, suggesting that those cytokines have a dramatic effect on the nerve microenvironment after PNI. To explore this further, PPI networks were constructed by uploading the up- and downregulated proteins into GeneMANIA. In addition to the differentially expressed proteins, other chemotactic and inflammatory factors were selected within these networks, such as CC chemokine ligand (CCL17), chemokine (C-X-C motif) ligand (CXCL13), the tissue inhibitor of metalloproteinases-3 (TIMP3) and others. At 1 day after PNI, the differentially expressed proteins were mainly related to chemotactic family proteins (CCL2, CCL3, CCL7, CCL17, CXCL2, CXCL3, CXCL6, CXCL9, CXCL11 and CXCL13) (**Figure 2A**). At 7 days after PNI, the proteins in the PPI included GFR alpha2, GFR alpha3, GFR alpha4, IL9, IL19, IL20, tyrosine-protein kinase 2 (JAK 2), Jag1, Jag2, TIMP3, TIMP4, VEGFB, GDNF, Neurturin (NRTN) (**Figure 2B**). At 14 days after PNI, CCL1, CCL2, CCL5, CCL7, CCL15, CXCL1, CXCL2, intercellular adhesion molecule 2 (ICAM2), ICAM4, ICAM5, GFR alpha1, GDNF family receptor (GFR) alpha2, GFR alpha4, Notch-3, Galectin-1, Galectin-2, Galectin-5, Galectin-12 were selected in the PPI network (**Figure 2C**). At 28 days after PNI, GFR alpha2, GFR alpha3, GFR alpha4, Notch-3, VEGFB, GDNF, NRTN, placenta growth factor, TIMP2, TIMP3, TIMP4, ICAM1, ICAM2, ICAM4, ICAM5, Galectin-12, GTPase Hras, Jag2 interacted with the differentially expressed proteins (**Figure 2D**). In addition, there were several connections between the differentially expressed proteins and the selected proteins. Co-expression characteristics and described physical interactions accounted for most of the aforementioned targets and their interacting proteins. Other results, including shared protein domains, co-localization and predictions are shown in **Figure 2**.

Kyoto Encyclopedia of Genes and Genomes enriched analysis of integrated metabolic pathways following sciatic nerve injury

The proteins from the PPI networks were correlated with integrated metabolic pathways using KEGG analysis in DAVID. The top 10 canonical pathways associated with differentially expressed cytokines at each time point were displayed and analyzed using a *P*-value threshold of 0.05 (**Figure 3**). Cytokine-cytokine receptor interactions and rheumatiod arthritis were activated throughout the entire post-injury period. Notably, the chemokine signaling pathways, Janus kinase/signal transducers and activators of transcription (JAK/STAT) and phosphoinositide 3-kinase/protein kinase B (PI3K/Akt), and leishmainasis were drastically stimulated at 1–7 days after PNI, while the notch signaling pathway and dorso-ventral axis formation were enriched at 14–28 days after PNI. Besides, malaria and influenze A were activited at 1–14 days after PNI. A full list of the canonical pathways and their involved molecules identified at 1, 7, 14, and 28 days after PNI is provided in **Additional Table 1**.

Gene ontology analysis of biological processes following sciatic nerve injury

To further explore the effects of cytokines following sciatic nerve injury, GO analysis was performed in DAVID to analyze biological processes. The top 10 biological processes (*P*

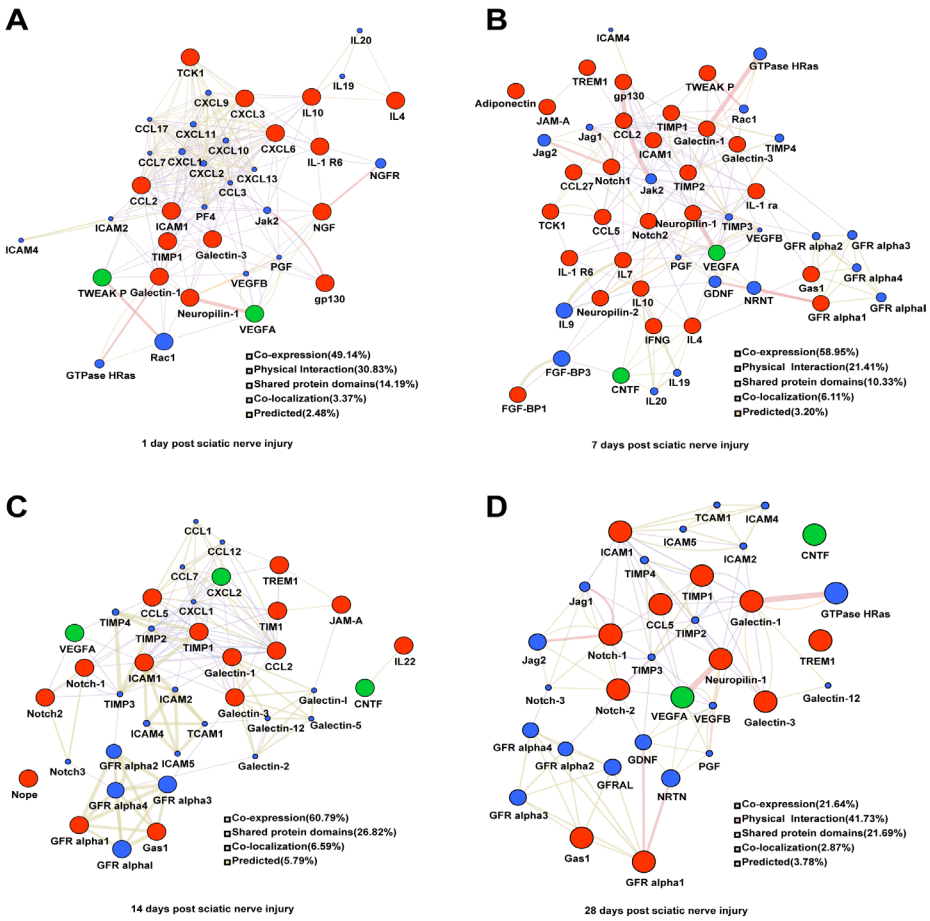

Figure 2 Networks of protein-protein interactions of the differentially expressed proteins in the distal nerve stump following sciatic nerve transection.

(A–D) Differentially expressed proteins at 1 (A), 7 (B), 14 (C), 28 (D) days. The sizes of the spots in the network represent the weights of the interaction involving the protein. The red spots represent the upregulated proteins and green spots the downregulated proteins at each time point after sciatic nerve transection. The blue spots represent the selected proteins interact with the differentially expressed proteins. The colors of the the connecting lines represent the different interactions between protein and protein. The thickness of the connecting lines represents the score of each connection.

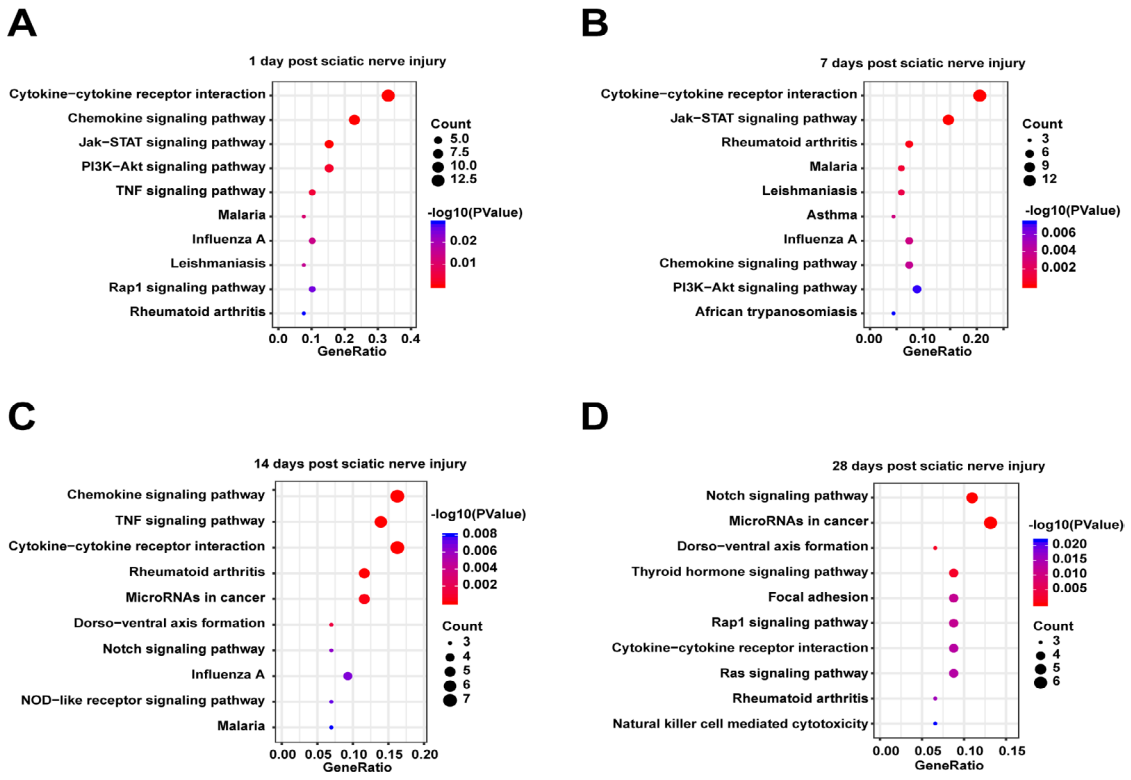

Figure 3 Kyoto Encyclopedia of Genes and Genomes (KEGG) pathways enriched among the proteins in the protein-protein interaction network in the distal nerve stump following sciatic nerve transection.

(A–D) Differentially expressed proteins at 1 (A), 7 (B), 14 (C) and 28 (D) days. The top 10 KEGG pathways with $P < 0.05$ are listed. The x-axis represents the gene ratio, defined as the ratio of the numbers of differentially expressed proteins to all proteins annotated in the KEGG pathway using Database for Annotation, Visualization, and Integrated Discovery (DAVID; http://www.david.niaid.nih.gov).

< 0.05) associated with these proteins are displayed in **Figure 4**. At 1–7 days after PNI, biological processes related to inflammation, the immune response, and cell chemotaxis were activated. At 14 days after PNI, even more cell chemotaxis processes, as well as cell response to IL-1, interferon-gamma were activated, including neutrophil, monocyte, lymphocyte, and eosinophil chemotaxis. At 28 days after PNI, neuronal apoptotic processes, cell-cell adhesion, and cell proliferation were enriched. However, some biological processes were negatively regulated at different time after PNI. For example, the negative regulation of apoptosis first increased at 1–7 days after PNI, and then progressively declined at 14 days after PNI, before increasing again at 28 days after PNI. Membrane protein ectodomain proteolysis was inhibited from 7–28 days after PNI. Catalytic activity reduced at 7 and 28 days after PNI. A full list of the biological processes and involved molecules at 1, 7, 14, and 28 days after PNI is provided in **Additional Table 2**. More information on the highly enriched cellular components associated with PNI associated with the external side of the plasma membrane, extracellular matrix, immunological synapse, and receptor complex are shown in **Additional Table 3**.

The relationships between proteins and functional terms in the distal nerve stump following sciatic nerve transection

The identified cytokines seem to affect many functional pathways and PPI networks via direct and indirect interactions. Therefore, to visualize smaller high-dimensional data subsets, the relationships between functional terms and differentially expressed proteins were assessed using the GOplot package in R (Walter et al., 2015) to integrate the expression data with the results of these analyses. Monocyte chemoattractant protein-1 (MCP-1/CCL2) regulated upon activation of normal T cell expressed and secreted (RANTES)/CCL5 and Galectin-3 that are related to monocyte and neutrophil chemotaxis, whereas CNTF and GDNF are specific to neuronal apoptotic processes. Notch1, Notch2, and Galectin-3 may participate in cell differentiation during nerve regeneration (**Figure 5**). Additionally, inflammatory responses involve many cytokines, including CCL2, CCL17, CXCL2, CXCL9, CXCL11, CXCL13, NGFR, GDNF, IL10, IL20, and IL19 (**Figure 5**).

Western blot verification of the protein array results in the distal nerve stump following sciatic nerve transection

Western blot analysis was performed to validate the temporal expression patterns of the differentially expressed growth factors in the nerves identified in the microarray analyses. Western blot analysis confirmed that CNTF expression levels decreased markedly, whereas GDNF and HGF were increased after PNI (**Figure 6A** & **B**), similar to the results of microarray analyses (**Figure 6C**).

Discussion

Wallerian demyelination is the most typical cause of PNI, resulting in a series of complicated cellular responses and molecular mechanisms. Numerous studies have demonstrated that PNI induces cytokine production in immune and non-immune cells at sites distal to the nerve lesion (Karanth et al., 2006; Kiguchi et al., 2017). Such cytokines are closely related to Wallerian demyelination and participate in peripheral nerve regeneration (Rotshenker, 2011; He et al., 2016; Lin et al., 2019). In the current study protein microarray and bioinformatic analyses were performed to examine the detailed kinetic changes in cytokine production in distal nerve stumps following sciatic nerve injury.

In this study, the 67 cytokines on the protein microarray comprise growth factors, chemotaxis factors, and other proteins. By screening differentially expressed cytokines after PNI, we discovered that some growth factors may be critical for sciatic nerve injury and regeneration. For instance, previous studies reported that GFR alpha-1 is expressed in myelinated peripheral nerves and the neuromuscular junction, exerting its effects on motor neurons by interacting with GDNF (Hase et al., 1999; Rosich et al., 2017). In line with previous findings, we detected upregulation of GFR alpha-1 protein at 7, 14, and 28 days after PNI. Additionally, HGF also increased 1.5-fold at 28 days post injury. HGF has been shown to promote the migration and proliferation of Schwann cells and increase the expression of neurotrophic factors and inflammatory cytokines such as GDNF and tumor necrosis factor-α (Ko et al., 2018). In contrast, we found that CNTF was downregulated over most of the post-injury period studied. The PPI network suggested that CNTF regulates neuronal apoptosis via the JAK/STAT signaling pathway. All of these results highlight the central roles of growth factors in nerve regeneration.

Chemokine factors have been identified as important modulators of peripheral nerve regeneration (Taskinen and Röyttä, 2000). MCP-1/CCL2, a CCL family member, is expressed at low levels under basal conditions and is upregulated rapidly and markedly in Schwann cells and neurons (Schreiber et al., 2001; Tanaka et al., 2004; Niemi et al., 2013). In this study, we found that MCP-1 expression increased 10-fold from 1 to 28 days after sciatic nerve injury. Consequently, the injury-induced increase in MCP-1 may lead to recruitment of inflammatory monocytes and macrophages to nerves via the Toll-like receptor-4 or STAT3-dependent signaling pathways (Niemi et al., 2013). Moreover, other CCL family members, including RANTES/CCL5, cutaneous T-cell-attracting chemokine (CTACK)/CCL27 were also upregulated at different time points after PNI. RANTES/CCL5 is another important chemokine that exhibits strong chemoattractant activity towards monocytes and leukocytes, inducing immune cell migration and protection of neurons, either directly or indirectly (Raport et al., 1996; Tillie-Leblond et al., 2000; Tokami et al., 2013; Solga et al., 2015). CTACK was reported to accelerate skin regeneration via specific chemokine-receptor interactions (Inokuma et al., 2006), suggesting an important role of CTACK in nerve regeneration.

Notch proteins (Notch-1–4) are transmembrane receptors that regulate cellular processes, including cell proliferation, apoptosis, and angiogenesis (Bolós et al., 2007; Fortini, 2009;

Kopan and Ilagan, 2009). During nerve regeneration, notch signaling mediates the differentiation of adipose-derived stem cells into Schwann-like cells and of monocytes into macrophages (Ohishi et al., 2001; Kingham et al., 2009). In our study, both Notch-1 and -2 were upregulated and may play important roles in the differentiation of the nervous system. It is also worth noting that Neuropilin-1 was upregulated from 1 to 28 days and Neuropilin-2 within 7 days after PNI. These proteins are closely related to axonal guidance, angiogenesis, and motor neuron migration. Triggering receptor expressed on myeloid cells 1 (TREM1) is another protein involved in immune response signaling pathways (Collins et al., 2009; Kingham et al., 2009) and activation of TREM1 may increase the secretion of pro-inflammatory cytokines (Walter, 2016). TREM1 continually increased over the time period we examined and was related to neutrophil chemotaxis. These results suggest that a cytokine network is involved in the kinetics of macrophage recruitment and nerve removal of damaged nerves.

Bioinformatic analyses are efficient methods for interpreting proteomic or genomic information. PPI network bioinformatic data are used to predict protein functionality within sequence homology clusters (Athanasios et al., 2017). Chemotactic factors, immune factors, and other cytokines were identified in our PPI network. Thymus and activation-regulated chemokine (TARC)/CCL17 accelerates fibroblast migration and wound healing (Kato et al., 2011). Rac GTPase, together with mammalian T-cell lymphoma invasion, metastasis factor 1 (TIAM-1) and CDC42, has been shown to mediate axon guidance (Demarco et al., 2012). These proteins may participate in nerve regeneration directly or indirectly. Additionally, the KEGG pathways resulted in the cytokine-cytokine receptor interactions keeping active during Wallerian degeneration. Other enriched pathways included the JAK/STAT, PI3K/Akt, and chemokine signaling pathways. Furthermore, our study demonstrated a diverse array of biological processes, including chemotaxis, inflammatory and immune responses, cell migration, cell proliferation, apoptosis, and angiogenesis, that were significantly activated in the distal nerve stump following sciatic nerve transection. Based on the relationships between cytokines and our bioinformatic data, further in-depth studies are needed to determine the detailed mechanism of peripheral nerve regeneration.

In summary, we analyzed global changes in cytokine expression patterns at the distal nerve stump following PNI using protein microarray analysis. Although our results did not elucidate the mechanism of PNI, bioinformatic analysis enabled us to gain a comprehensive view of cytokine expression changes with time. They also show the relationships of these cytokines with canonical pathways, biological functions, and networks during Wallerian degeneration. Overall, our study may help identify the potential clinic treatments for PNI.

Author contributions: *Study design: XQC, XZL, AJS, JP; experiments performing: XQC, GHH, SW, XD, PL, XS, QQ, HT; data analysis: XQC, XZL; manuscript writing: XQC; manuscript revising: QZ, AJS, JP. All authors approved the final version of the paper.*

Conflicts of interest: *The authors declare that there is no conflict of interests regarding the publication of this paper.*

Financial support: *This study was supported by the National Key Research & Development Program of China, No. 2017YFA0104702 (to AJS), and the National Basic Research Program of China (973 Program), No. 2014CB542201 (to JP). The funders had no involvement in the study design; data collection, analysis, and interpretation; paper writing; or decision to submit the paper for publication.*

Institutional review board statement: *This study was approved by the Institutional Animal Care and Use Committee of the Chinese PLA General Hospital (approval No. 2016-x9-07) in September 2016.*

Copyright license agreement: *The Copyright License Agreement has been signed by all authors before publication.*

Data sharing statement: *Datasets analyzed during the current study are available from the corresponding author on reasonable request.*

Plagiarism check: *Checked twice by iThenticate.*

Peer review: *Externally peer reviewed.*

Additional files:

Additional Table 1: *All canonical pathways and involved molecules at 1, 7, 14, and 28 days after sciatic nerve injury.*

Additional Table 2: *All biological function categories and involved molecules at 1, 7, 14, and 28 days after sciatic nerve injury.*

Additional Table 3: *All cellular component categories and involved molecules at 1, 7, 14, and 28 days after sciatic nerve injury.*

References

Athanasios A, Charalampos V, Vasileios T, Ashraf GM (2017) Protein-protein interaction (PPI) network: recent advances in drug discovery. Curr Drug Metab 18:5-10.

Bolós V, Grego-Bessa J, de la Pompa JL (2007) Notch signaling in development and cancer. Endocr Rev 28:339-363.

Chen ZL, Yu WM, Strickland S (2007) Peripheral regeneration. Annu Rev Neurosci 30:209-233.

Clements MP, Byrne E, Camarillo Guerrero LF, Cattin AL, Zakka L, Ashraf A, Burden JJ, Khadayate S, Lloyd AC, Marguerat S, Parrinello S (2017) The wound microenvironment reprograms Schwann cells to invasive mesenchymal-like cells to drive peripheral nerve regeneration. Neuron 96:98-114.e7.

Collins CE, La DT, Yang HT, Massin F, Gibot S, Faure G, Stohl W (2009) Elevated synovial expression of triggering receptor expressed on myeloid cells 1 in patients with septic arthritis or rheumatoid arthritis. Ann Rheum Dis 68:1768-1774.

da Costa CC, van der Laan LJ, Dijkstra CD, Bruck W (1997) The role of the mouse macrophage scavenger receptor in myelin phagocytosis. Eur J Neurosci 9:2650-2657.

Demarco RS, Struckhoff EC, Lundquist EA (2012) The Rac GTP exchange factor TIAM-1 acts with CDC-42 and the guidance receptor UNC-40/DCC in neuronal protrusion and axon guidance. PLoS Genet 8:e1002665.

Dennis G Jr, Sherman BT, Hosack DA, Yang J, Gao W, Lane HC, Lempicki RA (2003) DAVID: Database for annotation, visualization, and integrated discovery. Genome Biol 4:P3.

Fortini ME (2009) Notch signaling: the core pathway and its posttranslational regulation. Dev Cell 16:633-647.

Frostick SP, Yin Q, Kemp GJ (1998) Schwann cells, neurotrophic factors, and peripheral nerve regeneration. Microsurgery 18:397-405.

Geuna S, Raimondo S, Ronchi G, Di Scipio F, Tos P, Czaja K, Fornaro M (2009) Chapter 3: Histology of the peripheral nerve and changes occurring during nerve regeneration. Int Rev Neurobiol 87:27-46.

Hase A, Suzuki H, Arahata K, Akazawa C (1999) Expression of human GFR alpha-1 (GDNF receptor) at the neuromuscular junction and myelinated nerves. Neurosci Lett 269:55-57.

He XZ, Wang W, Hu TM, Ma JJ, Yu CY, Gao YF, Cheng XL, Wang P (2016) Peripheral nerve repair: theory and technology application. Zhongguo Zuzhi Gongcheng Yanjiu 20:1044-1050.

Inokuma D, Abe R, Fujita Y, Sasaki M, Shibaki A, Nakamura H, McMillan JR, Shimizu T, Shimizu H (2006) CTACK/CCL27 accelerates skin regeneration via accumulation of bone marrow-derived keratinocytes. Stem Cells 24:2810-2816.

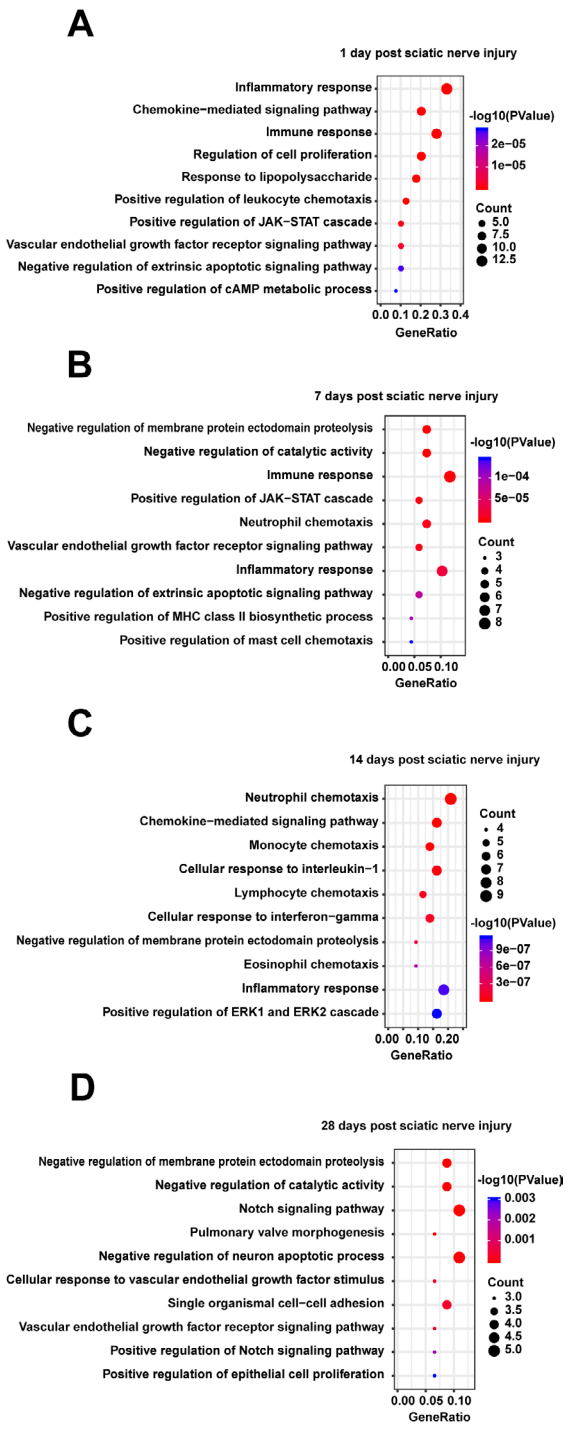

Figure 4 Gene ontology (GO) biological processes of those proteins enriched in the protein-protein interaction network in the distal nerve stump following sciatic nerve transection relative to all proteins.

(A–D) Differentially expressed proteins at 1 (A), 7 (B), 14 (C), 28 (D) days. The top 10 GO biological processes with $P < 0.05$ are listed. The x-axis represents the gene ratio, defined as the ratio of the numbers of differentially expressed proteins to all proteins annotated in the GO biological processes using Database for Annotation, Visualization, and Integrated Discovery (DAVID; http://www.david.niaid.nih.gov).

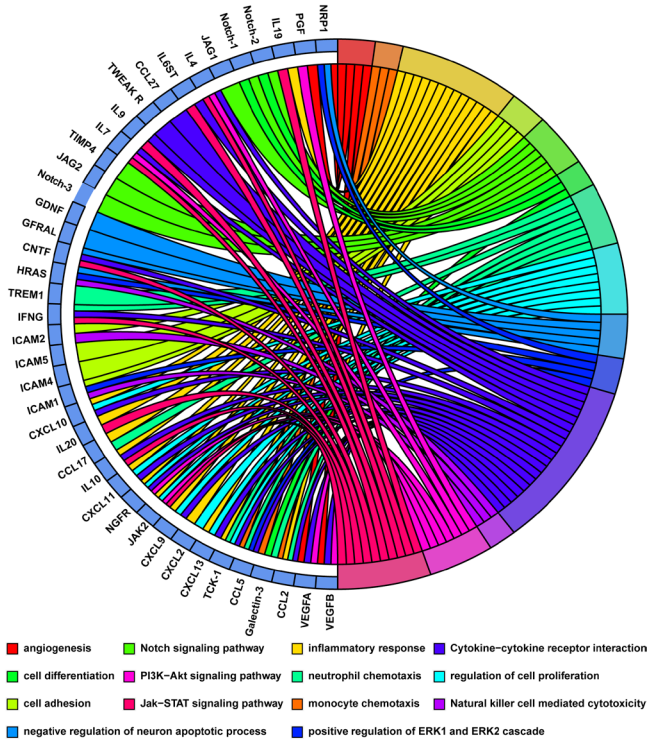

Figure 5 The relationship between the differentially expressed proteins and functional terms (biological processes and canonical pathways) in the distal nerve stump following sciatic nerve transection.

Multiple biological processes and canonical pathways are labeled by different colors in circles on the right. The proteins linked to each term are listed in circles on the left.

Karanth S, Yang G, Yeh J, Richardson PM (2006) Nature of signals that initiate the immune response during Wallerian degeneration of peripheral nerves. Exp Neurol 202:161-166.

Kato T, Saeki H, Tsunemi Y, Shibata S, Tamaki K, Sato S (2011) Thymus and activation-regulated chemokine (TARC)/CC chemokine ligand (CCL) 17 accelerates wound healing by enhancing fibroblast migration. Exp Dermatol 20:669-674.

Kiguchi N, Kobayashi D, Saika F, Matsuzaki S, Kishioka S (2017) Pharmacological regulation of neuropathic pain driven by inflammatory macrophages. Int J Mol Sci 18:E2296.

Kingham PJ, Mantovani C, Terenghi G (2009) Notch independent signalling mediates Schwann cell-like differentiation of adipose derived stem cells. Neurosci Lett 467:164-168.

Ko KR, Lee J, Lee D, Nho B, Kim S (2018) Hepatocyte growth factor (HGF) promotes peripheral nerve regeneration by activating repair schwann cells. Sci Rep 8:8316.

Kopan R, Ilagan MX (2009) The canonical Notch signaling pathway: unfolding the activation mechanism. Cell 137:216-233.

Lin YF, Xie Z, Zhou J, Yin G, Lin HD (2019) Differential gene and protein expression between rat tibial nerve and common peroneal nerve during Wallerian degeneration. Neural Regen Res 14:2183-2191.

Luck C, DeMarco VG, Mahmood A, Gavini MP, Pulakat L (2017) Differential regulation of cardiac function and intracardiac cytokines by rapamycin in healthy and diabetic rats. Oxid Med Cell Longev 2017:5724046.

Niemi JP, DeFrancesco-Lisowitz A, Roldan-Hernandez L, Lindborg JA, Mandell D, Zigmond RE (2013) A critical role for macrophages near axotomized neuronal cell bodies in stimulating nerve regeneration. J Neurosci 33:16236-16248.

Ohishi K, Varnum-Finney B, Serda RE, Anasetti C, Bernstein ID (2001) The Notch ligand, Delta-1, inhibits the differentiation of monocytes into macrophages but permits their differentiation into dendritic cells. Blood 98:1402-1407.

Pan B, Shi ZJ, Yan JY, Li JH, Feng SQ (2017) Long non-coding RNA NONMMUG014387 promotes Schwann cell proliferation after peripheral nerve injury. Neural Regen Res 12:2084-2091.

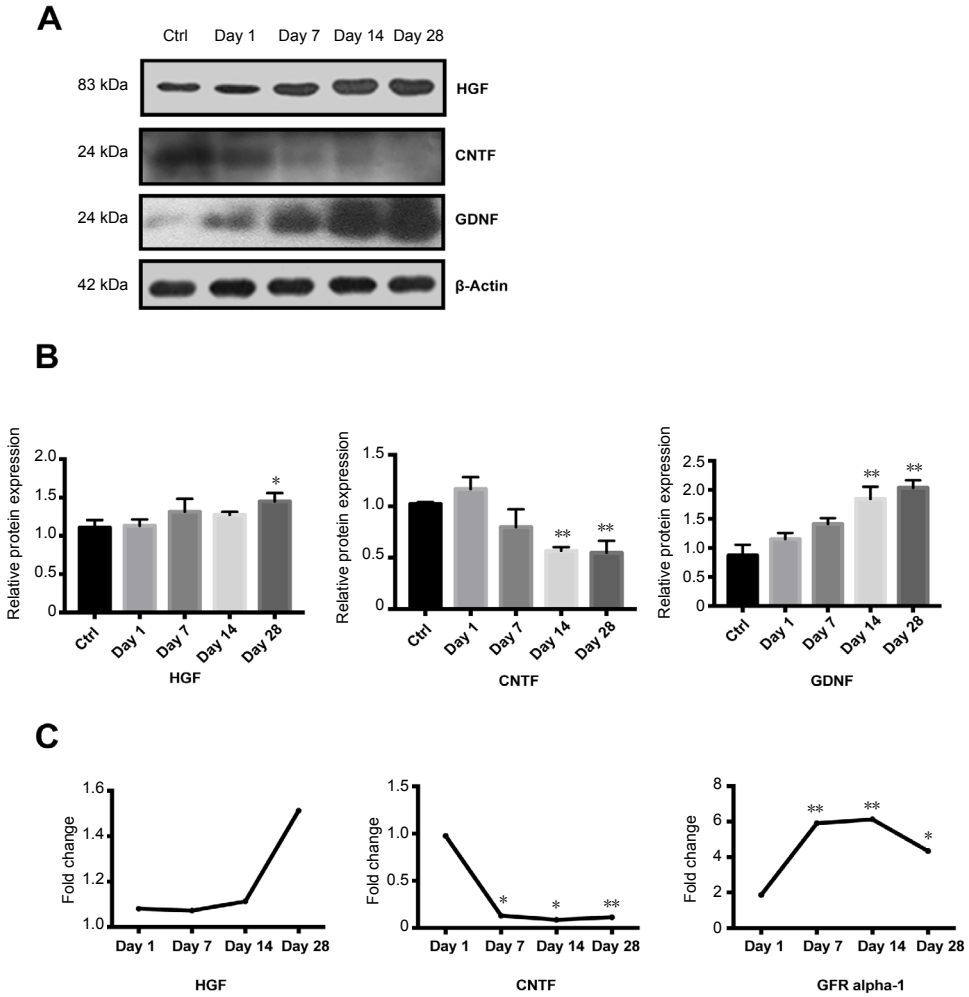

Figure 6 Western blot analyses of the differentially expressed growth factors in the distal nerve stump following sciatic nerve transection.

(A) Protein bands of HGF, CNTF and GDNF were measured by Western blot analysis. β-Actin was used as the reference protein. (B) Quantitative result of HGF, CNTF and GDNF expression. (C) The fold changes of HGF, CNTF and GFR alpha-1 were measured by protein microarray. Data represent the mean ± SEM (n = 4) from three independent experiments, statistically analyzed by one-way analysis of variance followed by Tukey's *post hoc* test. $*P < 0.05$, $**P < 0.01$, *vs.* control group (ctrl; 0 day after nerve injury). CNTF: Ciliary neurotrophic factor; GDNF: glial cell line-derived neurotrophic factor; HGF: hepatocyte growth factor.

Raimondo S, Fornaro M, Tos P, Battiston B, Giacobini-Robecchi MG, Geuna S (2011) Perspectives in regeneration and tissue engineering of peripheral nerves. Ann Anat 193:334-340.

Raport CJ, Gosling J, Schweickart VL, Gray PW, Charo IF (1996) Molecular cloning and functional characterization of a novel human CC chemokine receptor (CCR5) for RANTES, MIP-1beta, and MIP-1alpha. J Biol Chem 271:17161-17166.

Rosich K, Hanna BF, Ibrahim RK, Hellenbrand DJ, Hanna A (2017) The effects of glial cell line-derived neurotrophic factor after spinal cord injury. J Neurotrauma 34:3311-3325.

Rotshenker S (2011) Wallerian degeneration: the innate-immune response to traumatic nerve injury. J Neuroinflammation 8:109.

Schreiber RC, Krivacic K, Kirby B, Vaccariello SA, Wei T, Ransohoff RM, Zigmond RE (2001) Monocyte chemoattractant protein (MCP)-1 is rapidly expressed by sympathetic ganglion neurons following axonal injury. Neuroreport 12:601-606.

Siebert H, Sachse A, Kuziel WA, Maeda N, Bruck W (2000) The chemokine receptor CCR2 is involved in macrophage recruitment to the injured peripheral nervous system. J Neuroimmunol 110:177-185.

Solga AC, Pong WW, Kim KY, Cimino PJ, Toonen JA, Walker J, Wylie T, Magrini V, Griffith M, Griffith OL, Ly A, Ellisman MH, Mardis ER, Gutmann DH (2015) RNA sequencing of tumor-associated microglia reveals Ccl5 as a stromal chemokine critical for neurofibromatosis-1 glioma growth. Neoplasia 17:776-788.

Takahashi K, Prinz M, Stagi M, Chechneva O, Neumann H (2007) TREM2-transduced myeloid precursors mediate nervous tissue debris clearance and facilitate recovery in an animal model of multiple sclerosis. PLoS Med 4:e124.

Tanaka T, Minami M, Nakagawa T, Satoh M (2004) Enhanced production of monocyte chemoattractant protein-1 in the dorsal root ganglia in a rat model of neuropathic pain: possible involvement in the development of neuropathic pain. Neurosci Res 48:463-469.

Taskinen HS, Röyttä M (2000) Increased expression of chemokines (MCP-1, MIP-1alpha, RANTES) after peripheral nerve transection. J Peripher Nerv Syst 5:75-81.

Tillie-Leblond I, Hammad H, Desurmont S, Pugin J, Wallaert B, Tonnel AB, Gosset P (2000) CC chemokines and interleukin-5 in bronchial lavage fluid from patients with status asthmaticus. Potential implication in eosinophil recruitment. Am J Respir Crit Care Med 162:586-592.

Tokami H, Ago T, Sugimori H, Kuroda J, Awano H, Suzuki K, Kiyohara Y, Kamouchi M, Kitazono T; REBIOS Investigators (2013) RANTES has a potential to play a neuroprotective role in an autocrine/paracrine manner after ischemic stroke. Brain Res 1517:122-132.

van der Laan LJ, Ruuls SR, Weber KS, Lodder IJ, Dopp EA, Dijkstra CD (1996) Macrophage phagocytosis of myelin in vitro determined by flow cytometry: phagocytosis is mediated by CR3 and induces production of tumor necrosis factor-alpha and nitric oxide. J Neuroimmunol 70:145-152.

Walter J (2016) The triggering receptor expressed on myeloid cells 2: a molecular link of neuroinflammation and neurodegenerative diseases. J Biol Chem 291:4334-4341.

Walter W, Sánchez-Cabo F, Ricote M (2015) GOplot: an R package for visually combining expression data with functional analysis. Bioinformatics 31:2912-2914.

Webber C, Zochodne D (2010) The nerve regenerative microenvironment: early behavior and partnership of axons and Schwann cells. Exp Neurol 223:51-59.

Yi S, Tang X, Yu J, Liu J, Ding F, Gu X (2017) Microarray and qPCR analyses of wallerian degeneration in rat sciatic nerves. Front Cell Neurosci 11:22.

Yi S, Zhang H, Gong L, Wu J, Zha G, Zhou S, Gu X, Yu B (2015) Deep sequencing and bioinformatic analysis of lesioned sciatic nerves after crush injury. PLoS One 10:e0143491.

Yu B, Zhou S, Wang Y, Qian T, Ding G, Ding F, Gu X (2012) miR-221 and miR-222 promote Schwann cell proliferation and migration by targeting LASS2 after sciatic nerve injury. J Cell Sci 125:2675-2683.

Yu J, Gu X, Yi S (2016) Ingenuity pathway analysis of gene expression profiles in distal nerve stump following nerve injury: insights into wallerian degeneration. Front Cell Neurosci 10:274.

C-Editor: Zhao M; S-Editors: Yu J, Li CH; L-Editors: Yu J, Song LP; T-Editor: Jia Y

Category	Term	Count	%	*P*-value	Molecules	List total	Pop hits	Pop total	Fold enrichmen	Bonferroni	Benjamini	FDR
Day 1												
KEGG_PATHWAY	ssc04060:Cytokine-cytokine receptor interaction	13	0.33121019	3.40E-13	VEGFB, IL4, CCL2, PPBP, IL6ST, TNFRSF12A, CXCL13, VEGFA, CXCL9, NGFR, CXCL11, IL10,	23	221	7030	17.97953964	2.04E-11	2.04E-11	3.40E-10
KEGG_PATHWAY	ssc04062:Chemokine signaling pathway	9	0.22929936	2.73E-08	CCL2, PPBP, CXCL13, CXCL2, CXCL9, JAK2, CXCL11, CCL17, CXCL10	23	173	7030	15.90098015	1.64E-06	8.18E-07	2.73E-05
KEGG_PATHWAY	ssc04630:Jak-STAT signaling pathway	6	0.15286624	5.85E-05	IL4, IL6ST, IL19, JAK2, IL10, IL20	23	140	7030	13.09937888	0.003500988	0.00116836	0.05856165
KEGG_PATHWAY	ssc04151:PI3K-Akt signaling pathway	6	0.15286624	0.00285045	IL4, VEGFB, PGF, VEGFA, JAK2, NGFR	23	326	7030	5.625500133	0.157406886	0.04191404	2.820171
KEGG_PATHWAY	ssc04668:TNF signaling pathway	4	0.10191083	0.00439045	ICAM1, CCL2, CXCL2, CXCL10	23	108	7030	11.32045089	0.232031866	0.05143163	4.31383707
KEGG_PATHWA	ssc05144:Malaria	3	0.07643312	0.01127811	ICAM1, CCL2, IL10	23	52	7030	17.63377926	0.493652212	0.1072261	10.7445415
KEGG_PATHWA	ssc05164:Influenza A	4	0.10191083	0.0145511	ICAM1, CCL2, JAK2, CXCL10	23	167	7030	7.321010154	0.585001467	0.11806775	13.6617584
KEGG_PATHWA	ssc05140:Leishmanias	3	0.07643312	0.01578332	IL4, JAK2, IL10	23	62	7030	14.78962132	0.615015566	0.11247541	14.7376045
KEGG_PATHWAY	ssc04015:Rap1 signaling pathway	4	0.10191083	0.02533146	VEGFB, PGF, VEGFA, NGFR	23	206	7030	5.934993668	0.785505085	0.15722237	22.6735405
KEGG_PATHWAY	ssc05323:Rheumatoid arthritis	3	0.07643312	0.02916058	ICAM1, CCL2, VEGFA	23	86	7030	10.66228514	0.830627048	0.16269361	25.6646135
KEGG_PATHWAY	ssc04014:Ras signaling pathway	4	0.10191083	0.03002464	VEGFB, PGF, VEGFA, NGFR	23	220	7030	5.557312253	0.8394382	0.15319063	26.3249811
KEGG_PATHWAY	ssc04620:Toll-like receptor signaling pathway	3	0.07643312	0.03917298	CXCL9, CXCL11, CXCL10	23	101	7030	9.078777443	0.909068921	0.18110913	32.9997956
KEGG_PATHWA	ssc05310:Asthma	2	0.05095541	0.06965828	IL4, IL10	23	23	7030	26.57844991	0.986861379	0.28340618	51.4995559
Day 7												
KEGG_PATHWAY	ssc04060:Cytokine-cytokine receptor interaction	14	0.20548951	2.8045E-13	IL4, CCL2, IL7, TNFRSF12A, IL6ST, IL9, CCL5, CCL27, IL10, VEGFB, CNTF, PPBP, VEGFA, IFNG	28	221	7030	15.90497738	2.04723E-11	2.0472E-11	2.9272E-10
KEGG_PATHWAY	ssc04630:Jak-STAT signaling pathway	10	0.14677822	1.3162E-09	IL4, CNTF, IL6ST, IL7, IFNG, IL19, IL9, JAK2, IL10, IL20	28	140	7030	17.93367347	9.60815E-08	4.8041E-08	1.3738E-06
KEGG_PATHWAY	ssc05323:Rheumatoid arthritis	5	0.07338911	0.00029559	ICAM1, CCL2, IFNG, VEGFA, CCL5	28	86	7030	14.59717608	0.021350158	0.00716798	0.30810644
KEGG_PATHWA	ssc05144:Malaria	4	0.05871129	0.00098511	ICAM1, CCL2, IFNG, IL10	28	52	7030	19.31318681	0.06942148	0.0178264	1.02348937
KEGG_PATHWA	ssc05140:Leishmanias	4	0.05871129	0.00164329	IL4, IFNG, JAK2, IL10	28	62	7030	16.19815668	0.113131722	0.02372577	1.70201483
KEGG_PATHWA	ssc05310:Asthma	3	0.04403347	0.00341977	IL4, IL9, IL10	28	23	7030	32.7484472	0.221254387	0.04082187	3.51247659
KEGG_PATHWA	ssc05164:Influenza A	5	0.07338911	0.00351799	ICAM1, CCL2, IFNG, JAK2, CCL5	28	167	7030	7.51710864	0.226837364	0.0360851	3.61169015
KEGG_PATHWAY	ssc04062:Chemokine signaling pathway	5	0.07338911	0.00399326	CCL2, PPBP, JAK2, CCL5, CCL27	28	173	7030	7.25639967	0.253300018	0.03585297	4.0904725
KEGG_PATHWAY	ssc04151:PI3K-Akt signaling pathway	6	0.08806693	0.00722646	IL4, VEGFB, PGF, IL7, VEGFA, JAK2	28	326	7030	4.620946538	0.411069421	0.05713054	7.29086559
KEGG_PATHWAY	ssc05143:African trypanosomiasis	3	0.04403347	0.00738845	ICAM1, IFNG, IL10	28	34	7030	22.15336134	0.418043509	0.0526967	7.44864556

KEGG_PATHWAY	ssc05142:Chagas disease (American trypanosomiasis)	4	0.05871129	0.00768878	CCL2, IFNG, CCL5, IL10	28	107	7030	9.385847797	0.430758015	0.04993293	7.74051304
KEGG_PATHWAY	ssc05330:Allograft rejection	3	0.04403347	0.00870947	IL4, IFNG, IL10	28	37	7030	20.35714286	0.471956101	0.05182354	8.72625592
KEGG_PATHWAY	ssc04330:Notch signaling pathway	3	0.04403347	0.0121687	NOTCH2, JAG2, JAG1	28	44	7030	17.11850649	0.590887078	0.06644097	11.9966412
KEGG_PATHWAY	ssc05321:Inflammatory bowel disease (IBD)	3	0.04403347	0.02261767	IL4, IFNG, IL10	28	61	7030	12.34777518	0.811761955	0.11244886	21.2421676
KEGG_PATHWAY	ssc05168:Herpes simplex infection	4	0.05871129	0.03164347	CCL2, IFNG, JAK2, CCL5	28	182	7030	5.518053375	0.904374051	0.14485771	28.5113284
KEGG_PATHWAY	ssc04066:HIF-1 signaling pathway	3	0.04403347	0.05684533	IFNG, VEGFA, TIMP1	28	101	7030	7.457567185	0.986050678	0.23434245	45.7127052
KEGG_PATHWAY	ssc04660:T cell receptor signaling pathway	3	0.04403347	0.06191833	IL4, IFNG, IL10	28	106	7030	7.105795148	0.990590483	0.24002715	48.684362
KEGG_PATHWAY	ssc04668:TNF signaling pathway	3	0.04403347	0.0639902	ICAM1, CCL2, CCL5	28	108	7030	6.974206349	0.991993018	0.23523844	49.8551108
KEGG_PATHWAY	ssc05145:Toxoplasmosis	3	0.04403347	0.07034613	IFNG, JAK2, IL10	28	114	7030	6.607142857	0.995130845	0.24440856	53.2975516
KEGG_PATHWAY	ssc05162:Measles	3	0.04403347	0.09057419	IL4, IFNG, JAK2	28	132	7030	5.706168831	0.999022737	0.29286788	62.8793488
Day 14												
KEGG_PATHWAY	rno04062:Chemokine signaling pathway	7	0.16252612	1.88E-06	CXCL1, CCL1, CCL12, CCL2, CXCL2, CCL5, CCL7	19	177	7780	16.19387452	7.92E-05	7.92E-05	1.74E-03
KEGG_PATHWAY	rno04668:TNF signaling pathway	6	0.1393081	3.65E-06	CXCL1, ICAM1, CCL12, CCL2, CXCL2, CCL5	19	109	7780	22.53983583	1.53E-04	7.66E-05	3.38E-03
KEGG_PATHWAY	rno04060:Cytokine-cytokine receptor interaction	7	0.16252612	6.00E-06	CCL12, CCL2, CNTF, VEGFA, CCL5, IL22, CCL7	19	216	7780	13.26998051	2.52E-04	8.40E-05	5.55E-03
KEGG_PATHWAY	rno05323:Rheumatoid arthritis	5	0.11609009	4.53E-05	ICAM1, CCL12, CCL2, VEGFA, CCL5	19	90	7780	22.74853801	1.90E-03	4.75E-04	4.19E-02
KEGG_PATHWAY	rno05206:MicroRNAs in cancer	5	0.11609009	2.74E-04	NOTCH3, NOTCH2, NOTCH1, VEGFA, TIMP3	19	143	7780	14.31726169	1.14E-02	2.30E-03	2.53E-01
KEGG_PATHWAY	rno04320:Dorso-ventral axis formation	3	0.06965405	1.47E-03	NOTCH3, NOTCH2, NOTCH1	19	25	7780	49.13684211	5.99E-02	1.02E-02	1.35E+00
KEGG_PATHWAY	rno04330:Notch signaling pathway	3	0.06965405	6.26E-03	NOTCH3, NOTCH2, NOTCH1	19	52	7780	23.62348178	2.32E-01	3.70E-02	5.65E+00
KEGG_PATHWAY	rno05164:Influenza A	4	0.09287207	6.68E-03	ICAM1, CCL12, CCL2, CCL5	19	171	7780	9.578331794	2.45E-01	3.46E-02	6.01E+00
KEGG_PATHWAY	rno04621:NOD-like receptor signaling pathway	3	0.06965405	7.23E-03	CCL12, CCL2, CCL5	19	56	7780	21.93609023	2.63E-01	3.33E-02	6.50E+00
KEGG_PATHWAY	rno05144:Malaria	3	0.06965405	8.00E-03	ICAM1, CCL12, CCL2	19	59	7780	20.82069581	2.86E-01	3.32E-02	7.17E+00
KEGG_PATHWAY	rno05142:Chagas disease (American trypanosomiasis)	3	0.06965405	2.48E-02	CCL12, CCL2, CCL5	19	107	7780	11.48057059	6.52E-01	9.16E-02	2.08E+01

KEGG_PATHWAY	rno04919:Thyroid hormone signaling pathway	3	0.06965405	2.84E-02	NOTCH3, NOTCH2, NOTCH1	19	115	7780	10.6819222	7.02E-01	9.59E-02	2.34E+01
KEGG_PATHWAY	rno04514:Cell adhesion molecules	3	0.06965405	5.90E-02	ICAM1, F11R, ICAM2	19	172	7780	7.141982864	9.22E-01	1.78E-01	4.30E+01
KEGG_PATHWAY	rno05168:Herpes simplex infection	3	0.06965405	8.78E-02	CCL12, CCL2, CCL5	19	216	7780	5.687134503	9.79E-01	2.41E-01	5.73E+01
Day 28												
KEGG_PATHWAY	cfa04330:Notch signaling pathway	5	0.10957703	3.4697E-06	NOTCH3, NOTCH2, NOTCH1, JAG2, JAG1	17	47	6781	42.43429287	2.64E-04	0.00026366	3.65E-03
KEGG_PATHWAY	cfa05206:MicroRNAs in cancer	6	0.13149244	1.2266E-05	NOTCH3, NOTCH2, NOTCH1, HRAS, VEGFA, TIMP3	17	139	6781	17.21794329	9.32E-04	0.000466	1.29E-02
KEGG_PATHWAY	cfa04320:Dorso-ventral axis formation	3	0.06574622	0.0017703	NOTCH3, NOTCH2, NOTCH1	17	27	6781	44.32026144	1.26E-01	0.04389487	1.85E+00
KEGG_PATHWAY	cfa04919:Thyroid hormone signaling pathway	4	0.08766163	0.00215415	NOTCH3, NOTCH2, NOTCH1, HRAS	17	113	6781	14.11972931	1.51E-01	0.04014488	2.24E+00
KEGG_PATHWAY	cfa04510:Focal adhesion	4	0.08766163	0.01170373	VEGFB, HRAS, PGF, VEGFA	17	207	6781	7.707871554	5.91E-01	0.16384884	1.17E+01
KEGG_PATHWAY	cfa04015:Rap1 signaling pathway	4	0.08766163	0.01170373	VEGFB, HRAS, PGF, VEGFA	17	207	6781	7.707871554	5.91E-01	0.16384884	1.17E+01
KEGG_PATHWAY	cfa04060:Cytokine-cytokine receptor interaction	4	0.08766163	0.01313391	VEGFB, CNTF, VEGFA, CCL5	17	216	6781	7.38671024	6.34E-01	0.15419378	1.30E+01
KEGG_PATHWAY	cfa04014:Ras signaling pathway	4	0.08766163	0.01346491	VEGFB, HRAS, PGF, VEGFA	17	218	6781	7.318942256	6.43E-01	0.13686453	1.33E+01
KEGG_PATHWAY	cfa05323:Rheumatoid arthritis	3	0.06574622	0.01553142	ICAM1, VEGFA, CCL5	17	82	6781	14.59325681	6.96E-01	0.13817783	1.52E+01
KEGG_PATHWAY	cfa04650:Natural killer cell mediated cytotoxicity	3	0.06574622	0.02174666	ICAM1, HRAS, ICAM2	17	98	6781	12.21068427	8.12E-01	0.16944791	2.07E+01
KEGG_PATHWAY	cfa04151:PI3K-Akt signaling pathway	4	0.08766163	0.0420905	VEGFB, HRAS, PGF, VEGFA	17	337	6781	4.73450864	9.62E-01	0.27878282	3.64E+01
KEGG_PATHWAY	cfa05200:Pathways in cancer	4	0.08766163	0.06126129	VEGFB, HRAS, PGF, VEGFA	17	392	6781	4.070228091	9.92E-01	0.35388619	4.86E+01
KEGG_PATHWAY	cfa05205:Proteoglycans in cancer	3	0.06574622	0.07581922	HRAS, VEGFA, TIMP3	17	195	6781	6.136651584	9.98E-01	0.39308589	5.64E+01
KEGG_PATHWAY	cfa05219:Bladder cancer	2	0.04383081	0.09257318	HRAS, VEGFA	17	41	6781	19.45767575	9.99E-01	0.4332909	6.40E+01

Category	Term	Count	%	*P*-value	Molecules	List total	Pop hits	Pop total	Fold enrichmen	Bonferroni	Benjamini	FDR
Day 1												
GOTERM_CC_DIRECT	GO:0005615~extracellular space	20	0.50955414	5.00E-19	IL4, ICAM1, NRP1, CCL2, LGALS3, PGF, LGALS1, CXCL2, IL19, CXCL9, CXCL11, IL10, IL20, CCL17, TIMP1, CXCL10, VEGFB, PPBP, CXCL13, VEGFA	26	762	12833	12.95477488	1.85E-17	1.85E-17	4.49E-16
GOTERM_CC_DIRECT	GO:0009897~external side of plasma membrane	5	0.12738854	7.90E-05	IL4, ICAM1, IL6ST, CXCL9, CXCL10	26	120	12833	20.56570513	0.00291951	0.00146082	0.07092918
GOTERM_CC_DIRECT	GO:0001772~immunological synapse	2	0.05095541	0.04576193	ICAM1, LGALS3	26	24	12833	41.13141026	0.82327447	0.43882313	34.3348902
GOTERM_CC_DIRECT	GO:0016020~membrane	5	0.12738854	0.04595763	VEGFB, PGF, ICAM2, VEGFA,	26	707	12833	3.49064302	0.8246105	0.35285604	34.4557081
Day 7												
GOTERM_CC_DIRECT	GO:0005615~extracellular space	23	0.3375899	1.4551E-17	IL4, ICAM1, CCL2, NRP1, LGALS3, PGF, IL7, LGALS1, IL9, IL1RN, IL19, TIMP4, TIMP2, CCL5, TIMP3, IL10, IL20, TIMP1, VEGFB, CNTF, PPBP, IFNG, VEGFA	40	762	12833	9.683694226	6.1114E-16	6.1114E-16	1.3467E-14
GOTERM_CC_DIRECT	GO:0009897~external side of plasma membrane	5	0.07338911	0.00046445	IL4, ICAM1, IL6ST, IFNG, GFRA3	40	120	12833	13.36770833	0.01932219	0.00970822	0.42902184
GOTERM_CC_DIRECT	GO:0005578~proteinaceous extracellular matrix	5	0.07338911	0.00087497	LGALS1, TIMP4, TIMP2, TIMP3, TIMP1	40	142	12833	11.29665493	0.03609734	0.0121802	0.80686791
GOTERM_CC_DIRECT	GO:0005576~extracellular region	7	0.10274475	0.00131741	NRTN, IL7, ADIPOQ, GDNF, FGFBP1, CCL27, TIMP1	40	407	12833	5.517874693	0.053863	0.01374662	1.21265635
GOTERM_CC_DIRECT	GO:0005622~intracellular	6	0.08806693	0.03118422	VEGFB, CCL2, GFRAL, LGALS1, IFNG, GFRA2	40	586	12833	3.284897611	0.73567964	0.23365183	25.4130934
GOTERM_CC_DIRECT	GO:0001772~immunological synapse	2	0.02935564	0.07050482	ICAM1, LGALS3	40	24	12833	26.73541667	0.95361474	0.40058169	49.1690919
GOTERM_CC_DIRECT	GO:0005604~basement membrane	2	0.02935564	0.08457142	TIMP3, TIMP1	40	29	12833	22.12586207	0.97555289	0.41149956	55.8597181
Day 14												
GOTERM_CC_DIRECT	GO:0005615~extracellular space	21	0.48757836	2.2092E-15	CXCL1, CCL1, ICAM1, HAVCR1, CCL2, ICAM4, LGALS3, LGALS1, CXCL2, TIMP4, CCL5, TIMP2, TIMP3, IL22, CCL7, TIMP1, CCL12, CNTF, VEGFA, GFRA1, GFRA4	34	1316	18520	8.692115144	1.5099E-13	1.5099E-13	2.2871E-12
GOTERM_CC_DIRECT	GO:0005578~proteinaceous extracellular matrix	6	0.1393081	7.9388E-05	LGALS3, LGALS1, TIMP4, TIMP2, TIMP3, TIMP1	34	253	18520	12.91792606	0.00538405	0.00269566	0.08164213
GOTERM_CC_DIRECT	GO:0009986~cell surface	8	0.18574414	8.3982E-05	ICAM1, NOTCH2, NOTCH1, HAVCR1, LGALS3, LGALS1, VEGFA, TIMP2	34	612	18520	7.120338331	0.00569472	0.00190185	0.0863644
GOTERM_CC_DIRECT	GO:0005604~basement membrane	4	0.09287207	0.00059964	VEGFA, TIMP2, TIMP3, TIMP1	34	93	18520	23.42820999	0.03996739	0.01014519	0.6151823
GOTERM_CC_DIRECT	GO:0043235~receptor complex	4	0.09287207	0.00165145	NOTCH3, NOTCH2, NOTCH1, GFRA1	34	132	18520	16.50623886	0.10630582	0.02222757	1.68599929

GOTERM_CC_DIRECT	GO:0031012~extracellular matrix	4	0.09287207	0.01026878	LGALS3, LGALS1, TIMP3, TIMP1	34	254	18520	8.578045391	0.50435096	0.11039808	10.0744937
GOTERM_CC_DIRECT	GO:0009897~external side of plasma membrane	4	0.09287207	0.01174935	ICAM1, LGALS3, GFRA1, GFRA3	34	267	18520	8.160387751	0.55232434	0.10846655	11.4488433
GOTERM_CC_DIRECT	GO:0005886~plasma membrane	14	0.32505224	0.01438302	F11R, ICAM1, LGALS3, ICAM4, GFRAL, ICAM5, ICAM2, GAS1, NOTCH3, NOTCH2, NOTCH1, GFRA1, GFRA4, GFRA3	34	3963	18520	1.924270087	0.62661575	0.11586313	13.8467933
GOTERM_CC_DIRECT	GO:0005623~cell	3	0.06965405	0.01898445	CXCL1, CCL12, CXCL2	34	119	18520	13.73208107	0.72838062	0.13481944	17.8960826
GOTERM_CC_DIRECT	GO:0005887~integral component of plasma membrane	6	0.1393081	0.02446583	ICAM1, NOTCH2, ICAM4, ICAM5, ICAM2, TCAM1	34	942	18520	3.469464219	0.81443802	0.1550152	22.495014
GOTERM_CC_DIRECT	GO:0070062~extracellular exosome	10	0.23218017	0.03763242	ICAM1, F11R, LGALS3, ICAM2, LGALS1, GFRA1, GFRA4, TIMP2, TIMP3, TIMP1	34	2646	18520	2.058601218	0.92634761	0.21110903	32.6067177
GOTERM_CC_DIRECT	GO:0001772~immunological synapse	2	0.04643603	0.05888631	ICAM1, LGALS3	34	34	18520	32.04152249	0.98386897	0.29101261	46.440432
GOTERM_CC_DIRECT	GO:0043025~neuronal cell body	4	0.09287207	0.07056971	CCL2, CNTF, GFRA1, TIMP2	34	540	18520	4.034858388	0.99310167	0.31805473	52.8997324
GOTERM_CC_DIRECT	GO:0031225~anchored component of membrane	2	0.04643603	0.09356231	GFRA1, GFRA4	34	55	18520	19.80748663	0.99874403	0.37943918	63.5997306
Day 28												
GOTERM_CC_DIRECT	GO:0005615~extracellular space	12	0.26298488	2.1928E-07	VEGFB, ICAM1, NRP1, CNTF, ICAM4, LGALS3, VEGFA, TIMP4, TIMP2, CCL5, TIMP3, TIMP1	29	814	13919	7.075658731	8.5518E-06	8.5518E-06	0.00019941
GOTERM_CC_DIRECT	GO:0005578~proteinaceous extracellular matrix	4	0.08766163	0.00409476	TIMP4, TIMP2, TIMP3, TIMP1	29	162	13919	11.85100043	0.14787636	0.07689457	3.6626419
GOTERM_CC_DIRECT	GO:0043235~receptor complex	3	0.06574622	0.01401283	NOTCH3, NOTCH2, NOTCH1	29	90	13919	15.99885057	0.42326116	0.16761087	12.0439761
GOTERM_CC_DIRECT	GO:0005887~integral component of plasma membrane	6	0.13149244	0.01431117	ICAM1, NOTCH2, ICAM4, ICAM5, ICAM2, JAG2	29	733	13919	3.928776403	0.43002802	0.13111284	12.2857025
GOTERM_CC_DIRECT	GO:0005912~adherens junction	2	0.04383081	0.04336572	NOTCH1, JAG1	29	22	13919	43.63322884	0.82254361	0.2923503	33.1802839
GOTERM_CC_DIRECT	GO:0001772~immunological synapse	2	0.04383081	0.05677946	ICAM1, LGALS3	29	29	13919	33.10107015	0.89769033	0.31611022	41.2328984
GOTERM_CC_DIRECT	GO:0005604~basement membrane	2	0.04383081	0.08676185	TIMP3, TIMP1	29	45	13919	21.33180077	0.97097463	0.3968896	56.1919967